한국기계가공학회지, 제20권, 제12호, pp. 54～65(2021.12) ISSN 1598-6721(Print)
Journal of the Korean Society of Manufacturing Process Engineers, Vol. 20, No. 12, pp. 54~65(2021.12) ISSN 2288-0771(Online)

https://doi.org/10.14775/ksmpe.2021.20.12.054

Internal Structure Optimization to enhance the Thermal Performance of an Air-cooled Lithium-ion Battery Pack

Quanyi Li*, Jong-Rae Cho*,#
*Dept. of Mechanical Engineering, Korea Maritime & Ocean University

공냉식 리튬 이온 배터리 팩의 열 성능 향상을 위한 내부 구조 최적화

Quanyi Li*, **조종래***,#
*한국해양대학교 대학원 기계공학과

(Received 20 July 2021; received in revised form 27 September 2021; accepted 08 October 2021)

ABSTRACT

Electric vehicles use lithium-ion battery packs as the power supply, where the batteries are connected in series or parallel. The temperature control of each battery is essential to ensure a consistent overall temperature. This study focused on reducing ohmic heating caused by batteries to realize a uniform battery temperature. The battery spacing was optimized to improve air cooling, and the tilt angle between the batteries was varied to optimize the internal structure of the batterypack. Simulations were performed to evaluate the effects of these parameters, and the results showed that the optimal scheme effectively achieved a uniform battery temperature under a constant power discharge. These findings can contribute to future research on cooling methods for battery packs.

Keywords: Lithium-ion Battery(리튬 이온 배터리), Battery Temperature(배터리 온도), Internal Structure(내부 구조), Tilt Angle(경사각), Temperature Uniformity(온도 균일성)

1. Introduction

Lithium-ion batteries (LIBs) have been receiving increased attention not only because of the environmental problems associated with the consumption of natural resources such as coal and petroleum but also their high-capacity density and service life. LIBs are an ideal alternative to nonrenewable fuel resources and play an important role in portable electronic devices in electric and hybrid electric vehicles[1-3]. However, some problems have been observed during the operation of systems using LIBs that correlate with thermal phenomena. In recent years, various researchers have focused on maintaining LIBs at an optimal operating temperature range of 20-45°C[4]. A higher temperature not only reduces the capacity but also may lead to thermal runaway of the LIB pack. Hence, a reasonable temperature management system is required to ensure that the LIB pack is in the optimal operating temperature range.

Cooling methods can be divided into active or passive; they include air cooling, liquid cooling, phase change materials (PCMs), and combinations of the

Corresponding Author : cjr@kmou.ac.kr
Tel: +82-51-410-4298, Fax: +82-51-405-4790

above[5]. Most methods in the literature for cooling the LIB pack focus on various ways to decrease the temperature while working with auxiliary means and provide constructive ideas for cooling optimization. Saw et al.[6] used an ultrasonic mist generator to provide cooling; this was able to maintain the maximum LIB temperature below 40°C with a temperature variation of less than 5°C for a charge rate of 3C. Zhou et al.[7] proposed a liquid cooling method based on a half-helical duct to maintain the operating temperature of a cylindrical LIB within the optimal range, and the optimal solution was found to effectively control the maximum temperature and temperature difference. Chen et al.[8] used multidisciplinary multi-objective design optimization to design a liquid cooling system that reduced the operating temperature and energy consumption. The temperature difference was controlled to within 0.35°C. Sun et al.[9] proposed the PCM-Fin system, which combines a PCM with novel fin structures. Their system not only increased the heat transfer area but also provided good thermal conduction within the PCM for effective control over the variation of the operating temperature. Zou et al.[10] developed a PCM composite comprising graphene, carbon tubes, and expanded graphite as the cooling media to enhance heat transfer characteristics. They kept the maximum temperature below 44.6°C and the maximum variation to 0.8°C for a 3C discharge rate. Yang et al.[11] proposed a novel distribution of expanded graphite–paraffin CPCM to minimize the temperature increase and maintain temperature uniformity for a 5C discharge rate. The optimal solution reduced the maximum temperature and its variation by 11.94% and 10.27%, respectively. An et al.[12] designed a novel thermal management system that coupled a paraffin (RT44HC)/expanded graphite CPCM with liquid cooling and found that the flow velocity plays an important role in the system. Their system provided a superior cooling effect compared to a pure PCM. Some researchers have focused on liquid cooling and PCMs for LIB packs, but most only considered auxiliary conditions such as heat exchangers, cold plates, and pumps in laboratory experiments, and the proposed methods increased the volume and weight of the LIB pack.

Meanwhile, manufacturers have focused on addressing the safety problems caused by coolant leakage during operation. For the LIB industry, reducing the energy consumption and cost are the main objectives for improving the cooling system of LIB packs. The volumetric energy density and gravimetric energy density are important measurement criteria. Compared to liquid cooling and PCM cooling, air cooling is a relatively mature technology and accords with the economic benefits highlighted by the industry.

To reduce the operating temperature, understanding how the system generates heat is important. The variation in temperature is caused by the interactions among heat from electrochemical reactions, ohmic heating, heat from side reactions, and heat from mixing[13]. Fig. 1 shows the reaction mechanism of a LIB, which demonstrates how it generates heat. The heat from side reactions and mixing can be neglected because their contribution to the total heat is insignificant. The total heat can be divided into two parts: reversible and irreversible. At a high discharge rate, most heat is irreversible; in contrast, reversible heat is dominant at a low discharge rate[14,5,2]. Most studies on the high operating temperature and cooling technology for LIBs have focused on mitigating the temperature variation by

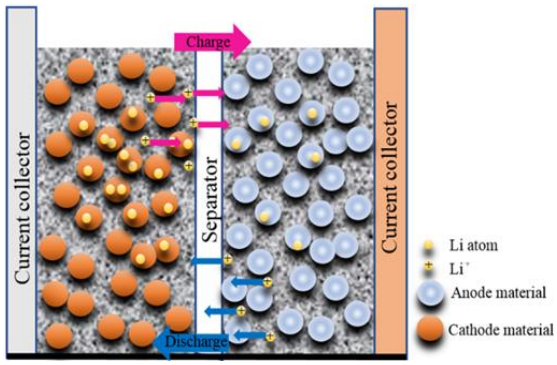

Fig. 1 Reaction mechanism of a working LIB

modifying the cooling method; however, few have considered reducing the amount of heat generated. Analyzing the source of the heat generation is important to maintain LIBs in the optimal operating temperature range. Some researchers have predicted heat generation by developing rational thermoelectric models or calculating the internal resistance of LIBs and the current in the electrodes[3,15,16]. Most of the total heat generation rate comprises the irreversible heating rate[5]. According to the research[3], the contact resistance between the current tab and cell body is the main factor leading to uneven battery temperature. however, few researches were reported on the optimization of ohmic heat source. Understanding how the main component of the heat occurs is important to developing novel measures at the link between the tab and cell body.

Motivated by the aforementioned research gaps, this study focused on cooling a LIB pack by mitigating the irreversible ohmic heating during charge and discharge. Thermal models were developed, and simulation experiments were performed. The results were analyzed to optimize the internal structure of the LIB pack for improved air flow and temperature uniformity. A prismatic LIB was considered to realize design parameters that satisfy reasonable standards, including the gravimetric energy density and volumetric energy density.

2. Thermal models

2.1 Heat generation model

The heat generation is determined by established a compete model to simulate the temperature variation of the prismatic battery under operation, as the internal heat generation has an influence on temperature distribution. It is essential to adopt reasonable heat generation mechanism. Despite electrode materials have many various categories, such as lithium iron phosphate, Lithium nickel cobalt manganate and so on, in which heat generation principle keeps consistently. Newman et al.[17] proposed the thermal model demonstrated in Eq. (1) to illustrate the heat generation.

$$q = I(V-U) + \frac{dU}{dT} + C_P\frac{dT}{dt} \tag{1}$$

Where q is the rate of total heat generation, I is the total current in the circuit, V is the terminal voltage, U is the open circuit voltage, T is the battery temperature, C_P is the heat capacity of battery, t is the time.

In Eq. (1), the term $I(V-U)$ represents the irreversible heat including the ohmic heat and polarization heat expressed as q_{ir}, $\frac{dU}{dT}$ is the reversible electrochemical reaction heat. $C_P\frac{dT}{dt}$ Is the internal energy change, so the simplified equation is got:

$$q = I(V-U) + \frac{dU}{dT} \tag{2}$$

In the above Eq. (2), the V and U need to be solved in the simulation process with the suitable coupled electrical-thermal model selected. The resistance thermal model is employed to compute the heat generation under operation.

$$\eta_p = \Phi_{1,p} - \Phi_{2,p} - U_{e,p} \tag{3}$$

$$\eta_p = \Phi_{1,p} - \Phi_{2,p} - U_{e,p} \tag{4}$$

Where η_p and η_n respectively represent the positive and negative electrodes overpotential, which represents the difference between the electrode potential and its equilibrium potential under a current density. Φ_1 denotes the solid phase potential and Φ_2 is the liquid phase electricity. U_e is the equilibrium electrode potential, and the subscripts p and n refer to the positive and negative electrodes.

The potential drop occurring in the solid and liquid phase can be simplified to the relationship of linear battery ohmic resistance.

$$(\Phi_{1,p}-\Phi_{1,n})+(\Phi_{2,p}-\Phi_{2,n})=IR_o \quad (5)$$

Where R_o is the ohmic resistance in battery.

So q_{ir} can be indicated into the other way:

$$q_{ir}=I(V-U)=I^2R_o+I(\eta_p-\eta_n) \quad (6)$$

Where $(\eta_p-\eta_n)$ can be caused by the polarization resistance due to overpotential, so it can be expressed by the polarization resistance R_p.

$$\eta_p-\eta_n=IR_p \quad (7)$$

According to Eq. (7), the Eq. (6) can be modified into:

$$q_{ir}=I^2(R_o+R_p) \quad (8)$$

During operation, temperature uniformity has a significant influence on the capacity of LIBs. The main contributors are the irreversible ohmic heating and polarization resistance heat caused by the electrode potential deviating from its equilibrium value when the current flows over the electrode under big power. Irreversible ohmic heating is influenced by the material properties and structure of the LIB[19]. This study focused on ohmic heating; the polarization heat was considered as a constant.

2.2 Heat transfer model of LIBs

Heat transfer has three mechanisms: conduction, convection, and radiation[4,15]. Normally, LIBs have an operating temperature of less than 60°C; thus, the amount of radiation heat is low and was neglected for the heat transfer model[18,19]. This study considered air cooling, where convection is the primary heat transfer mechanism. Thus, conduction was also neglected for the heat transfer model. The convection heat transfer of a LIB is reflected by three factors: the convective heat transfer coefficient between the cooling air and cell body, the distribution of the LIB monomer in the LIB pack, and the convection heat transfer between the surface of the LIB pack and outside. Air cooling can be represented by the following expression:

$$\overrightarrow{\varnothing_q}=h\Delta T \quad (9)$$

where $\overrightarrow{\varnothing_q}$ is the heat flux, h is the convective heat transfer coefficient, and ΔT is the difference in temperature.

The model needed to be simplified to avoid complex simulations by simplifying the electrochemical reaction and heat generation in the discharge process. The following characteristics were assumed for the sake of simplicity: although the LIB components theoretically have different thermo-physical properties, each LIB was regarded as a homogenous body composed of spherical particles of equal size; the specific heat capacity and heat conduction property remain constant under different conditions; the heat transfer is isotropic; and conduction and radiation can be neglected; no chemical side reaction occurred under operation; the electrode layer only has solid-liquid phase reaction and no gas phase material was generation; the influence of potential difference in the collector was ignored.

3. Simulation experiment

3.1 Governing equations

Three-dimensional computational fluid dynamics (CFD) is used to simulate complex systems involving fluid flow, which is applicable to the cooling of LIBs. Performing physical experiments would be a complex undertaking that requires many pieces of auxiliary equipment and have high costs. Furthermore, errors caused by human factors can be easily introduced. Many studies have shown that CFD simulations return results that are consistent with those of actual experiments. Hence, CFD was adopted to optimize the operating conditions of a LIB pack. The simulation was performed in ANSYS Fluent 18.0, and the two-equation turbulence model ($k-\epsilon$) was adopted for the fluid flow because the cooling air is in a turbulent state.

For the model, the energy conversion of the air-cooled LIB was set as follows:

$$\frac{\partial}{\partial x}\left(k\frac{\partial T}{\partial x}\right)+\frac{\partial}{\partial y}\left(k\frac{\partial T}{\partial y}\right)+\frac{\partial}{\partial z}\left(k\frac{\partial T}{\partial z}\right)+q=\rho C_b\frac{\partial T}{\partial t} \tag{10}$$

where ρ is the average mass density, C_b and k are the specific heat and thermal conductivity coefficient, respectively, and q is the heat generation rate of the LIB.

The LIB temperature distribution was considered to simulate the operating conditions and was determined by the energy equation, momentum equation, and continuity equation. These are respectively given below:

$$\left(\frac{\partial}{\partial t}+\nabla v\right)\rho_a C_a T_a=\nabla\left(k_a\nabla T_a\right) \tag{11}$$

$$\rho_a\frac{dv}{dt}=-\nabla P+\mu\nabla^2 v \tag{12}$$

$$\rho_a\nabla v=\frac{\partial\rho_a}{\partial t} \tag{13}$$

where v is the velocity of air, ρ_a is the mass density of air, C_a is the heat capacity of air, k_a is the thermal conductivity coefficient, P is the static pressure, and μ is the dynamic viscosity of the cooling air.

The dimensions and thermophysical properties of the prismatic cells are listed in Table 1. The model was operated under constant power with above equations governing.

Table 1 Dimension and properties parameter used in simulation

Parameter	Value
Battery body (mm)	220×132×6.6
ρ (kg /m^3)	2719
C_b (J/kg K)	871
k (W/m K)	20
ρ_a (kg/m^3)	1.225
v (m/s)	20
C_a (J /kg K)	1006.43
k_a (W m-1 k-1)	0.0242
μ (kg m-1s-1)	1.7894e-05

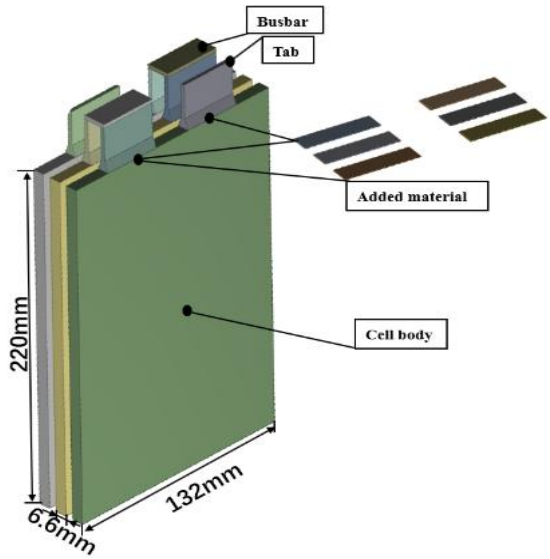

Fig. 2 Structure and dimensions of a single LIB

The maximum temperature and temperature difference were obtained through CFD simulations. The LIBs were discharged to exhaustion, so the transient solver was chosen. The SIMPLE method was selected to find the solution. The Green–Gauss node-based method was adopted for spatial discretization because it is more accurate than other approaches. The second-order method was used to discretize the pressure, and the second-order upwind method was used to discretize the momentum, turbulent kinetic energy, and turbulent dissipation rate.

3.2 Analysis of simulation for optimization

The simulation for optimization was performed according to the following steps:

(1) Ohmic heating was regarded as the main research object, so the position between the cell body and tab was optimized.

Meanwhile the battery pulse discharge was adopted to evaluate the contribution of polarization heat to the total heat.

According to Madani et al.[5], the total heat generated is almost the same as that generated by ohmic heating.

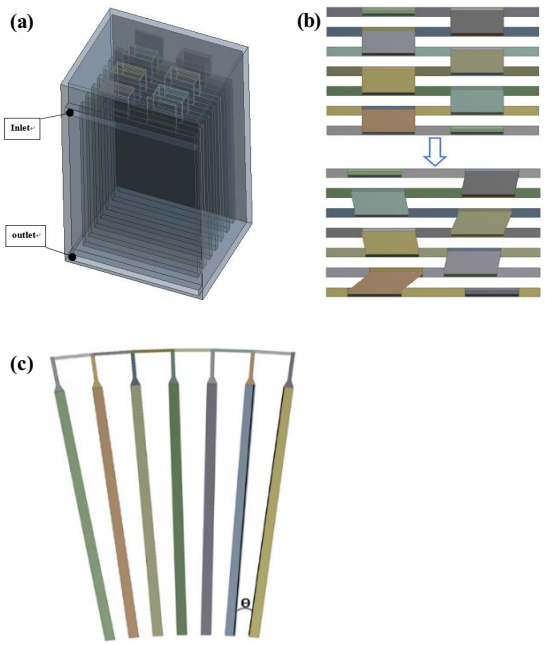

Fig. 3 Model for air-cooling optimization: (a) layout of the inlet and outlet, (b) change to the tab arrangement, and (c) tilt angle between LIBs

To smoothen the results, the copper material was added with preferred properties for the electrical conductivity and thermal conductivity. Fig. 2 shows the details. The thickness of the added material should be optimized considering the gravimetric energy density. At the same workload, diverse heat conditions can be obtained by varying the thickness of the added material to change the ohmic resistance.

(2) The volume of the LIB pack was optimized according to the volumetric energy density. Based on the relevant literature[20-22], the LIB spacing was initially set to 4 mm. The spacing was then varied to search for the optimum distance. A rational spacing design is beneficial for heat dissipation. Peng et al.[21] showed that having the inlet and outlet on the same side effectively reduces the maximum temperature of the LIB pack and improves the temperature uniformity. They also showed that the heat dissipation is more sensitive to the inlet vent height than the outlet vent height, according to the literature. Fig. 3(a) shows the layout of the inlet and outlet. An air-cooled module is adopted, which is based on the National Renewable Energy Lab in their previous work[23] and reduce computing resources to modify the number of batteries.

(3) Compared to a cylindrical LIB, prismatic LIBs are more sensitive to temperature un-uniformity. Keeping temperature differences short is pivotal to maintaining a uniform temperature. The layout of the inlet and outlet also affects the temperature. The above considerations were used to optimize the internal structure of the LIB pack. The airflow path has a significant influence on the air cooling of a LIB, so improving airflow was imperative. The aim of change of tab arrangement is to alter the path of airflow. Fig. 3 (b) and (c) show the optimization of the internal structure for air cooling. The tab arrangement which was determined by considering the size of cell body and tab, and spacing between LIBs were optimized by varying the tilt angle θ.

4. Results and Discussion

4.1 LIB performance indices

Four indices were used to evaluate the cooling effect and temperature uniformity of the LIB pack in different situations. $T_{\max}$ was the maximum temperature among LIBs, and ΔT was the temperature difference between LIBs. ξ was the space utility rate, which is the volume of a LIB divided by the total volume of the LIB pack. $T_{\max}$ was used to evaluate the cooling effect; a smaller value indicated a better cooling effect. ΔT was used to evaluate the temperature uniformity inside the LIB pack. A bigger value for ξ indicates better space utilization and higher volumetric energy density. σ was the standard deviation of the temperature and was used to assess the temperature difference.

4.2 Thermal analysis of added material

The maximum temperature and temperature difference

were obtained at the end of discharge. Different LIBs were simulated at a constant power discharge of 200W in different configuration states. Fig. 4 displayed the curve of potential change under battery pulse discharge. The polarization heat would be alleviated by this way so that the ohmic heat can be investigated. The added material helped improve the heat dispersion of the LIBs. Form Fig. 5(a) to 5(c) showed the contour plots of the static temperature. The highest temperature was at the joint between the cell body and tab for a 1P3S LIB pack. The initial temperature was 300 K. Without the added material, was 314 K and under battery pulse discharge the was 313.6K. It was found that the contribution of polarization heat was approximately 0.4K on the max temperature in the model during the discharge process. With 0.1mm of added material, T_{max} was 313.4 K with no cooling. Figs. 6(a) and 6(b) show that the positions of the maximum total heat generation and volumetric ohmic heating source agreed with that of the maximum temperature. Irreversible ohmic heating comprised most of the heating source in the case of a high-power discharge. Hence, adding material with excellent conductivity can effectively reduce the increase in temperature with ohmic heating.

The appropriate thickness of the added material should be determined according to the gravimetric energy density. The thickness of the added material was incremented from 0.01mm to 0.11mm in steps of 0.01mm. Fig. 7 shows the maximum and minimum temperatures of the LIB pack with each thickness. The maximum temperature was minimized at an added material thickness of 0.07mm. In addition, the temperature difference was relatively low at this thickness compared to the LIB without the added material. The connection between the cell body and tab had poor electron transition when the added material was thin. Meanwhile, the resistance of the added material increased with its thickness, which affected the heat generation of the LIB pack. Obtaining a reasonable thickness for the added material had a significant effect on .

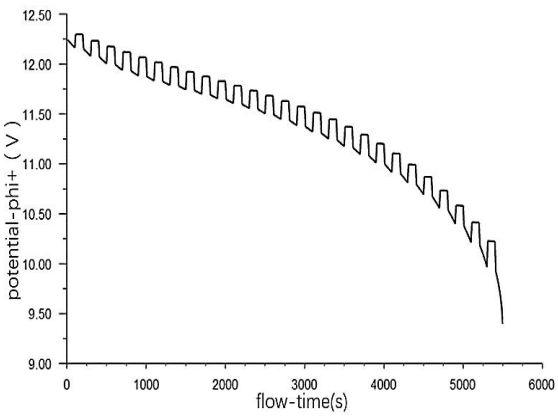

Fig. 4 Curve of potential changes under battery pulse discharge

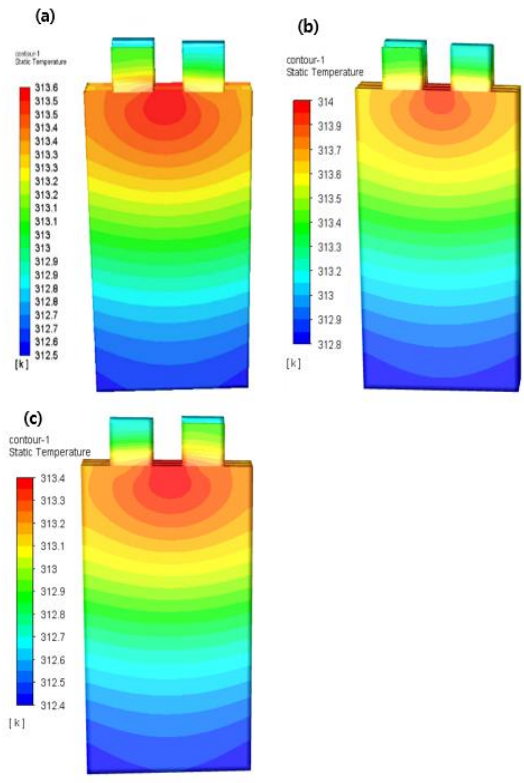

Fig. 5 Contour plot of static temperature of the 1P3S LIB pack: (a)under battery pulse discharge, (b)without added material, (c)with 0.1 mm thick added material

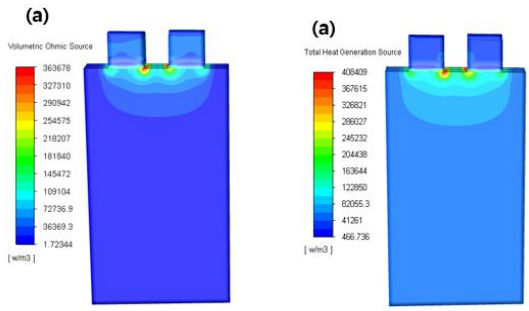

Fig. 6 Contour plot of (a) volumetric ohmic heating and (b) heat generation source of the LIB pack with the added material

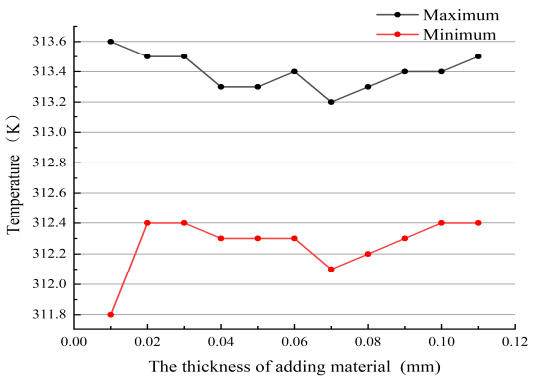

Fig. 7 Maximum and minimum temperatures with different thicknesses of the added material

4.3 Influence of the LIB spacing

LIB spacing is important to the cooling effect. In this study, it was evaluated according to ξ. The LIB spacing was varied to explore its influence on the operating temperature. Equal and unequal spacing distances were considered to determine their effects on T_{max} and ΔT. Figs. 8 depicts the temperature distribution and streamline of the cooling air. Appropriate spacing was found to lower the maximum temperature and help ensure a uniform temperature within a LIB pack. The path of the cooling air is shown by the streamline in Fig. 8(b). Most of the air exited along the tabs and then through cell 7; this is why cell 1 and cell 7 had lower temperatures than the other LIBs. The spacing was adjusted to increase the cooling effect as well as ξ and thus the volumetric energy density. Setting the spacing to 3.5mm improved ξ while maintaining the same T_{max} as the initial spacing of 4mm, as shown in Fig. 8(c). The maximum temperature increased when the spacing was increased from 4mm to 5.5mm. This was attributed to a slower airflow that reduced the heat dissipation efficiency. However, increasing the spacing to more than 5.5mm helped dissipate the heat generated during operation so the maximum temperature began to decrease. ΔT showed a similar trend as T_{max} it gradually decreased when the spacing was sufficient for heat dissipation, as shown in Fig. 8(c).

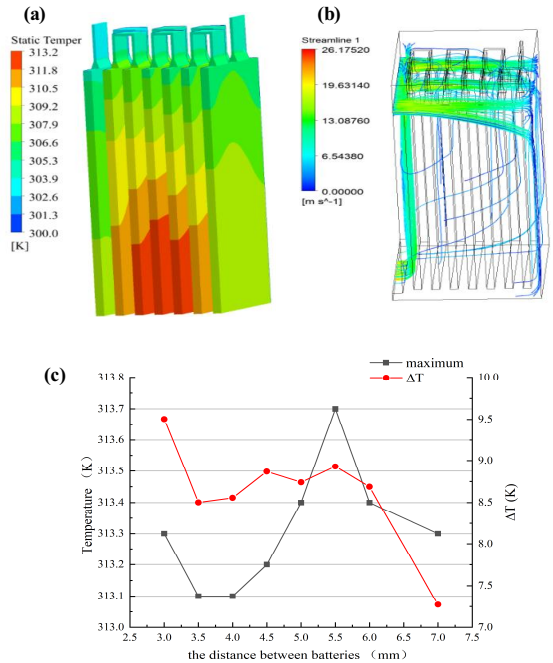

Fig. 8 (a) Temperature distribution of the 4 mm spacing, (b) internal air streamlines at the 4 mm spacing, and (c) maximum temperature and temperature difference with different spacing distances

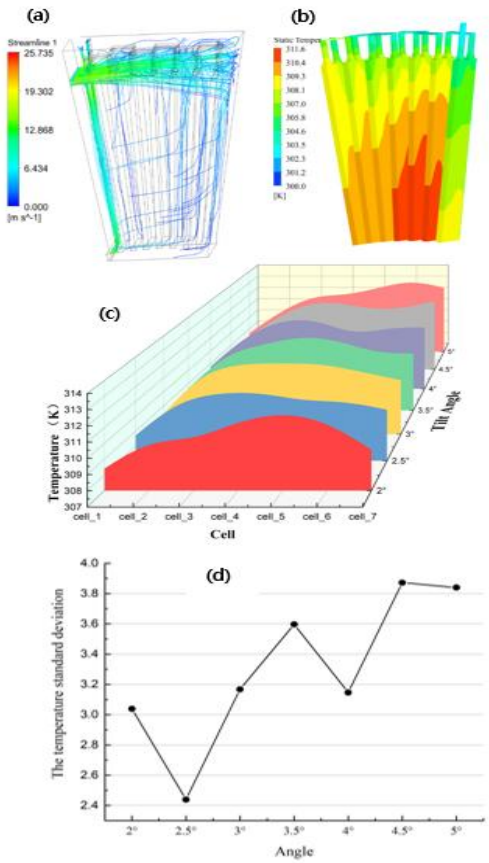

Fig. 9 (a) Streamlines of cooling airflow with the scattered tab arrangement, (b) static temperature distribution with a tilt angle of 2.5°, (c) maximum temperature of a single LIB at tilt angles of 2°~5°, and (d) standard deviation of the temperature at different tilt angles

4.4 Thermal analysis of the optimized internal structure

Depending on the airflow path in the interior, some of the air flows out along the edges of the LIBs and provides little cooling. Air streamlines were compared to identify the airflow path with the scattered tab arrangement, as shown in Fig. 9(a). The scattered tab arrangement helped distribute cooling air inside the LIB pack, which enhanced the temperature uniformity. The Tmax of LIB pack optimized by tab arrangement can be decreased than the LIB pack without optimization. In other words, the cooling air flowed through more areas when the flow rate was fixed, which improved heat dissipation.

The airflow speed increased in the tail along as the flow space was reduced. The cooling effect improved when the spacing between LIBs was gradually decreased from the inlet to the outlet, as shown in Fig. 3(c). This removed heat more quickly from LIBs near the outlet compared to the uniform parallel spacing configuration. Hence, the following tilt angles were spacing configuration. Hence, the following tilt angles were adopted: 2°, 2.5°, 3°, 3.5°, 4°, 4.5°, and 5°. The temperature distribution demonstrated that this configuration had a better cooling effect than the uniform spacing in Fig. 9(b). Fig. 9(c) shows that the temperature uniformity was better for a single LIB when the tilt angle was varied than when it was kept constant at 2.5°. The temperature difference of a single LIB in the same pack increased with the tilt angle. Increasing the spacing between LIBs changed the position of the maximum temperature when the tilt angle was greater than 2.5°. The maximum temperature migrated to the LIB far from the inlet because the increased distance affected the speed and temperature of the cooling air. This agrees with Fig. 8(c). At a relatively large distance from the head, the cooling air was not very hot, which was conducive for heat transfer. As the distance decreased, increasing the airflow rate increased the heat transfer coefficient. According to the standard deviation σ, the temperature uniformity of the LIB pack was optimized when the tilt angle was 2.5°, as shown in Fig. 9(d).

5. Conclusion

This study focused on optimizing the internal structure of a LIB pack with regarding to heat dissipation. Simulations were performed under the condition of constant power discharge to determine the changes in temperature of the LIBs. The results were

as follows:

(1) Ohmic heating dominates the total heat generation during operation and occurs at the junction between the cell body and tab; thus, adding special material is conducive to reducing the heat generation.

(2) The spacing between LIBs affects the temperature, and it can be optimized to improve the volumetric energy density of the LIB pack by choosing the reasonable distance between LIBs.

(3) The tab arrangement affects air cooling by changing the path of the airflow, and the dispersed airflow is more conductive to improve cooling . Meanwhile, the uniformity of temperature would be improved to ensure the safety of battery pack. And a suitable tilt angle optimizes the airflow area to improve temperature uniformity. The airflow rate near the bottom would be increased with the space decreasing so that the more heat would be taken away. A slight variation in temperature for a single LIB can affect the overall performance because a LIB pack comprises thousands of LIBs in parallel or series.

In future work, the results of this study can be extended to determine the optimal operating temperature range when air cooling is combined with liquid cooling or PCMs in different refrigerant types.

Acknowledgments

Authors would like to thank our colleagues Seongik Kim and Jinseong Park supporting help during simulation. All the authors promise that there is no conflict of interest in the study. This research did not receive any specific grant from funding agencies in the public, commercial.

References

1. Li, Q., Yang, Q., Zhao, Y., & Wan, B., "Carbon-based coating containing ultrafine MoO2 nanoparticles as an integrated anode for high-performance lithium-ion batteries", Journal of Nanoparticle Research, Vol. 19, No. 10, pp. 332, 2017.
2. Panchal, S., Mathew, M., Fraser, R., & Fowler, M., "Electrochemical thermal modeling and experimental measurements of 18650 cylindrical lithium-ion battery during discharge cycle for an EV", Applied Thermal Engineering, Vol. 135, No, 5, pp. 123, 2018.
3. Xie, Y., He, X.-j., Hu, X.-s., Li, W., Zhang, Y.-j., Liu, B., et al., "An improved resistance-based thermal model for a pouch lithium-ion battery considering heat generation of posts", Applied Thermal Engineering, Vol. 164, No. 1, pp. 114455, 2020.
4. Qian, X., Xuan, D., Zhao, X., & Shi, Z., "Heat dissipation optimization of lithium-ion battery pack based on neural networks", Applied Thermal Engineering, Vol. 162, No. 11, pp. 114289, 2019.
5. Madani, S. S., Swierczynski, M., & Kær, S. K., "Cooling simulation and thermal abuse modeling of lithium-ion batteries using the Newman", Tiedemann, Gu, and Kim (NTGK) model. ECS Transactions, Vol. 81, No. 1, pp. 261, 2017.
6. Saw, L. H., Poon, H. M., San Thiam, H., Cai, Z., Chong, W. T., Pambudi, N. A., et al., "Novel thermal management system using mist cooling for lithium-ion battery packs. Applied energy", Vol. 223, No. 8, pp. 146, 2018.
7. Zhou, H., Zhou, F., Zhang, Q., Wang, Q., & Song, Z. "Thermal management of cylindrical lithium-ion battery based on a liquid cooling method with half-helical duct", Applied Thermal Engineering, Vol. 162, No.11, pp. 114257, 2019.
8. Chen, S., Peng, X., Bao, N., & Garg, A. A., "comprehensive analysis and optimization process for an integrated liquid cooling plate for a prismatic lithium-ion battery module", Applied Thermal Engineering, Vol. 156, No. 6, pp. 324, 2019.
9. Sun, Z., Fan, R., Yan, F., Zhou, T., & Zheng, N., "Thermal management of the lithium-ion

battery by the composite PCM-Fin structures", International Journal of Heat and Mass Transfer, Vol. 145, No. 12, pp. 118739, 2019.

10. Zou, D., Liu, X., He, R., Zhu, S., Bao, J., Guo, J., et al., Preparation of a novel composite phase change material (PCM) and its locally enhanced heat transfer for power battery module, Energy Conversion and Management, Vol. 180, No. 1, pp. 1196, 2019.
11. Yang, M., Wang, H., Shuai, W., & Deng, X., "Thermal optimization of a kirigami-patterned wearable lithium-ion battery based on a novel design of composite phase change material", Applied Thermal Engineering, Vol. 161, No. 10, pp. 114141, 2019.
12. An, Z., Chen, X., Zhao, L., & Gao, Z., "Numerical investigation on integrated thermal management for a lithium-ion battery module with a composite phase change material and liquid cooling", Applied Thermal Engineering, Vol. 163, No. 12, pp. 114345, 2019.
13. Xie, Y., Shi, S., Tang, J., Wu, H., & Yu, J., "Experimental and analytical study on heat generation characteristics of a lithium-ion power battery", International Journal of Heat and Mass Transfer, Vol. 122, No. 7, pp. 884, 2018.
14. Cui, Y., Yang, J., Du, C., Zuo, P., Gao, Y., Cheng, X., et al., "Prediction Model and Principle of End-of-Life Threshold for Lithium Ion Batteries Based on Open Circuit Voltage Drifts", Electrochemical Acta, Vol. 255, No. 11, pp. 83, 2017.
15. Rizk, R., Louahlia, H., Gualous, H., & Schaetzel, P., "Experimental analysis and transient thermal modelling of a high capacity prismatic lithium-ion battery", International Communications in Heat and Mass Transfer, Vol. 94, No. 5, pp. 115, 2018.
16. Wang, C., Zhang, G., Meng, L., Li, X., Situ, W., Lv, Y., et al., "Liquid cooling based on thermal silica plate for battery thermal management system", International Journal of Energy Research, Vol. 41, No. 15, pp. 2468, 2017.
17. Thomas, K. E., & Newman, J., "Thermal modeling of porous insertion electrodes", Journal of The Electrochemical Society, Vol. 150, No. 2, pp. A176, 2003.
18. Putra, N., Ariantara, B., & Pamungkas, R. A., "Experimental investigation on performance of lithium-ion battery thermal management system using flat plate loop heat pipe for electric vehicle application", Applied Thermal Engineering, Vol. 99, No. 4, pp. 784, 2016.
19. Zhao, J., Rao, Z., & Li, Y., "Thermal performance of mini-channel liquid cooled cylinder based battery thermal management for cylindrical lithium-ion power battery", Energy Conversion and Management, Vol. 103, No. 10, pp. 157, 2015.
20. Li, W., Xiao, M., Peng, X., Garg, A., & Gao, L. A., "Surrogate thermal modeling and parametric optimization of battery pack with air cooling for EVs", Applied Thermal Engineering, Vol. 147, No. 1, pp. 90, 2019.
21. Peng, X., Ma, C., Garg, A., Bao, N., & Liao, X., "Thermal performance investigation of an air-cooled lithium-ion battery pack considering the inuniformity of battery cells", Applied Thermal Engineering, Vol. 153, No. 5, pp. 596, 2019.
22. Yu, X., Lu, Z., Zhang, L., Wei, L., Cui, X., & Jin, L., "Experimental study on transient thermal characteristics of stagger-arranged lithium-ion battery pack with air cooling strategy", International Journal of Heat and Mass Transfer, Vol. 143, No. 11, pp. 118576, 2019.
23. Fan, L., Khodadadi, J., & Pesaran, A. A., "Parametric study on thermal management of an air-cooled lithium-ion battery module for plug-in hybrid electric vehicles", Journal of Power Sources, Vol. 238, No. 9, pp. 301, 2013.